

Modeling of MHD waves in the solar corona

Pieter Luyten, Tomas Reunbrouck

April 30, 2020

Contents

1	Introduction	3
2	Theoretical background	4
2.1	Hydrodynamic fluid equations	4
2.2	Hydrodynamic linear waves	5
2.3	Hydrodynamic shocks	6
2.4	Magnetohydrodynamic fluid equations	8
2.5	Magnetohydrodynamic waves	10
2.5.1	Group speed	12
2.6	Units	14
3	Modeling shock waves	15
3.1	Hydrodynamic shockwave	15
3.2	Magnetohydrodynamic shock wave	18
4	Cornal hole	21

1 Introduction

The lay of the land

This report discusses simulation results of the plasma in the solar corona in accordance with the theory of magnetohydrodynamics (MHD). We aim give an qualitative interpretation of our simulation data based on the MHD equations for an ideal plasma.

Studying the behaviour of a plasma based on analytically acquired solutions of the MHD equations is very complicated. Thus, it is useful to attain some solutions numerically and interpret the results by means of visualizations.

In this manner we have completed an analysis of the behaviours of an idealised plasma for different boundary conditions. For each case we have investigated the influence of changes in the initial conditions by running the simulation in parallel for different values of the initial variables and comparing the outputs.

Physics of the solar corona

A brief justification of some basic assumptions is in place. As mentioned, we presuppose that the solar corona consists of an ideal plasma. That is, a highly ionised gas with smooth background conditions. A gas of this type should demonstrate a ‘collective behaviour’ which is necessary for the ideal MHD equations to be sufficiently accurate. By ‘collective behaviour’, we mean the following.

A plasma consists of positively charged ions and negatively charged electrons. To be able to assume the ideal MHD theory we must have that the kinetic energy of these particles sufficiently outweighs the potential energy produced by the pairwise Coulomb interactions. In other words, we require $\frac{KE}{PE} \gg 1$. If this is indeed the case we may presume that we are working with a collection of particles that interact on a smooth background.

Such a smooth background is achieved by a phenomenon called ‘electric screening’. This is the effect by which positively charged ions are electrically screened from each other - in that their mutual Coulomb interaction becomes negligible - by a surrounding cloud of electrons.

Consider any such ion. We can write its circumambient electric potential in a system of mobile charged particles as

$$\phi \sim \frac{1}{r} e^{-rk_D}$$

where $k_D = \frac{1}{\lambda_D}$ and λ_D is the Debye length. The reason why the Debye length is important for our purposes is that it traces the boundary of where the motion of the particles begins to outweigh the electric potential. We can see this because for a given electric charge Q

$$\frac{KE}{PE} \sim \frac{T}{\frac{Q}{\lambda_D}} \sim \frac{\lambda_{MFP}}{\lambda_D}$$

where λ_{MFP} is the mean length of a free particle path. This clarifies the significance of the strong inequality $\frac{KE}{PE} \gg 1$: the charged particles move quasi freely through the plasma with very infrequent occurrence of one to one electromagnetic interaction.

Since the temperature in the solar corona is of the order of $10^6 K$ we may assume that these ratios are sufficiently large to consider the ion gas as a collection of charged particles which behave collectively, which is what constitutes a plasma. [notes-principles-MHD]

Goal of this report

As mentioned, the main purpose of the project was to gain a basic understanding of the nature of the plasma in the solar corona. Specifically MHD waves are of great interest as they are directly observable in satellite observations of the sun. Therefore, we shall focus our report on them. Concretely, we discuss two compelling examples of MHD waves: the MHD blastwave and the interaction of an MHD wave with a coronal hole.

For the first problem we have simulated an MHD blastwave under the influence of a very powerful magnetic field. Visualizations of the output data have shown that the results are quite distinctive for different values of the magnetic field's strength. We have also simulated a blastwave under normal hydrodynamic conditions. This HD blastwave provides the case where the field strength is 0.

Secondly, we discuss a simulation where we had an MHD wave run into a coronal hole. This hole is part of the boundary conditions for this problem. It consists of a sharp drop in pressure and density. As one would expect, its effect on the wave is quite striking and we shall discuss it in detail.

The software used

The software that was used for the numerical solutions is called PLUTO. This is an open source code written specifically for the purpose of plasma simulations. It is a piece of code designed to solve the HD and MHD conservation laws for arbitrary initial conditions in a finite volume.

PLUTO was developed by the Department of Physics at Torino University. [[pluto-manual](#)]

2 Theoretical background

While the main focus of this project is the numerical modeling of waves in the solar corona, some theoretical background is important to frame the results of our simulations. Furthermore, this knowledge gives some insight in the assumptions that are made in deriving the magnetohydrodynamic (MHD) equations and when they are valid.

We shall begin by a discussion of the cleaner and more transparent theory of ideal hydrodynamics before delving into the much more complicated and cluttered realm of magnetohydrodynamic theory. However, we emphasize that there is no fine line between the two and that indeed, HD theory can be seen as the special case of MHD theory in with a negligible magnetic field.

2.1 Hydrodynamic fluid equations

The theory in this section is adapted from [[notes-fluid-dynamics](#)]. For the first task a non-viscous Newtonian fluid is considered. Heat conduction and dissipation is neglected as well. This type of fluid obeys the Euler equations for conservation of mass, momentum and internal energy:

$$\begin{aligned} \frac{d\rho}{dt} + \rho \nabla \cdot \mathbf{v} &= 0 \\ \rho \frac{d\mathbf{v}}{dt} &= -\nabla p + \mathbf{F} \\ \frac{dp}{dt} - \frac{\gamma p}{\rho} \frac{d\rho}{dt} &= 0 \end{aligned} \tag{1}$$

These are the Euler equations in Lagrangian form, with time derivatives following the fluid, hence the total derivatives with respect to time. PLUTO does the fluid simulation using a static grid. Therefore we need the equations in their Eulerian form: partial derivatives with respect to time instead of total derivatives. This change of derivatives can be carried out using the following relation, found in **[notes-fluid-dynamics]**, section 2.4:

$$\frac{df}{dt} = \frac{\partial f}{\partial t} + (\mathbf{v} \cdot \nabla)f \quad (2)$$

where $f(x, y, z, t)$ is a function that describes a property of the fluid. The resulting equations could also have been re-derived using an Eulerian view to begin with. In any case the result is the same:

$$\begin{aligned} \frac{\partial \rho}{\partial t} + \nabla \cdot (\rho \mathbf{v}) &= 0 \\ \frac{\partial}{\partial t}(\rho \mathbf{v}) &= \nabla \cdot (-p\mathbb{I} - \rho \mathbf{v} \mathbf{v}) + \mathbf{F} \\ \frac{\partial}{\partial t} \left(\rho \left(\frac{v^2}{2} + \mathcal{U} \right) \right) &= \mathbf{F} \cdot \mathbf{v} - \nabla \cdot \left(\rho \left(\frac{v^2}{2} + \mathcal{U} \right) \mathbf{v} + p \mathbf{v} \right) \end{aligned} \quad (3)$$

Next introduced is the variable $\mathbf{m} = \rho \mathbf{v}$, the momentum density. The energy density \mathcal{U} can be split in the thermal energy ρe and gravitational potential energy $\rho \Phi$. Let $E_t = e\rho + \frac{v^2}{2}$. The only external force is $\mathbf{F} = \rho \mathbf{g}$ carrying out these substitutions leads to the equations in section 6 in the PLUTO manual **[pluto-manual]**:

$$\begin{aligned} \frac{\partial \rho}{\partial t} + \nabla \cdot \mathbf{m} &= 0 \\ \frac{\partial \mathbf{m}}{\partial t} + \nabla \cdot (\mathbf{m} \mathbf{v} + p\mathbb{I}) &= -\rho \nabla \Phi + \rho \mathbf{g} \\ \frac{\partial}{\partial t} (E_t + \rho \Phi) + \nabla \cdot ((E_t + p + \rho \Phi) \mathbf{v}) &= \mathbf{m} \cdot \mathbf{g} \end{aligned} \quad (4)$$

These equations are soluble given an appropriate equation of state, expressing the thermal energy density ρe as a function of p and ρ . For the purpose of finding such an equation, assume the gas to be calorically ideal. That is, presuppose a constant number of degrees of freedom f for its constituent molecules. From this we extract the adiabatic constant:

$$\gamma = \frac{f+2}{f} \quad (5)$$

This expression which can be rewritten as

$$f = \frac{2}{\gamma - 1}$$

Finally, the necessary equation of state is found **[notes-fluid-dynamics][section 3.6.5]** :

$$\rho e = \frac{f}{2} n k_B T = \frac{p}{\gamma - 1}$$

Add a reference for this energy equation

short discussion of assumptions made (no viscosity and heat conduction, calorically ideal gas)

2.2 Hydrodynamic linear waves

We start again from the ideal fluid equations as given in eq. (3) and linearize them. For this we rewrite the quantities ρ and p as a background density ρ_0 and pressure p_0 with slight deviations ρ_1 ,

p_1 . Furthermore it is assumed that there are no external forces acting on the fluid. The Linearized equations are:

$$\begin{aligned} \frac{\partial \rho_1}{\partial t} + \rho_0 \nabla \cdot \mathbf{v} &= 0 \\ \rho_0 \frac{\partial \mathbf{v}}{\partial t} &= -\nabla p_1 \\ \frac{\partial p_1}{\partial t} &= \frac{\gamma p_0}{\rho_0} \frac{\partial \rho_1}{\partial t} \end{aligned} \quad (6)$$

By acting with ∇ on the second equation and using the first to substitute $\rho_0 \nabla \cdot \mathbf{v}$ we find the following relation:

$$\frac{\partial^2 \rho_1}{\partial t^2} = -\nabla^2 p_1$$

Acting with $\frac{\partial}{\partial t}$ on the last equation and substituting the previous expression yields

$$\frac{\partial^2 p_1}{\partial t^2} + \frac{\gamma p_0}{\rho_0} \nabla^2 p_1 = 0$$

which is the wave equation with speed

$$v_s = \sqrt{\frac{\gamma p_0}{\rho_0}} \quad (7)$$

the speed of sound in the ideal fluid, and the phase- and group speed of linear sound waves. Similar expressions are found for the other variables. this wave speed can be found by substituting a plane wave of the form $p_1 = A \exp(i(\omega t - \mathbf{k} \cdot \mathbf{x}))$. Substituting this expression in the wave equation for p_1 leads to the dispersion relation:

$$\omega^2 = k^2 v_s^2. \quad (8)$$

The group velocity is given by

$$\mathbf{v}_g = \frac{\partial \omega}{\partial \mathbf{k}} = v_s \hat{\mathbf{k}} \quad (9)$$

from which we conclude that these waves are non-dispersive.

Referentie?

reference for this relation for the group speed?

2.3 Hydrodynamic shocks

Now we shall reconsider one of the least convincing assumptions made for the derivations of the fluid equations: that of perfectly continuous background variables. In reality, we might encounter very sudden changes in the scalar variable density ρ and vectorial variable velocity \mathbf{v} . To have the theory of ideal fluids take this into account, we can introduce these jumps in the variables as mathematical discontinuities. This discontinuity is appropriately called a 'shock'. We are interested in how this shock moves through the fluid. The derivation of its motion is quite straight forward.

Start from the continuity equation in its Eulerian form in 1D

$$\frac{\partial \rho}{\partial t} + \frac{\partial(\rho v)}{\partial x} = 0 \quad (10)$$

Of course, this equation assumes that ρ and ρv are continuous variables with continuous partial derivatives. Rewrite the equation so that over a distance Δx and a duration Δt the variables ρ and ρv experience a change $\Delta \rho$ and $\Delta \rho v$. This gives the much less elegant version

$$\frac{\Delta \rho}{\Delta t} + \frac{\Delta(\rho v)}{\Delta x} = 0 .$$

If this were the perfectly continuous case we would now let $\Delta x, \Delta t \rightarrow 0$, resulting in eq. (10). However, we might also say that the transition is not smooth and that for $\Delta x, \Delta t \rightarrow 0$ the jump remains: $\Delta \rho, \Delta \rho v \rightarrow \Delta \rho, \Delta \rho v$. Rewrite the equations to see what this means:

$$\frac{\Delta x}{\Delta t} \Delta \rho + \Delta(\rho v) = 0 .$$

Then for $\Delta x, \Delta t \rightarrow 0$ we get

$$\frac{\partial x}{\partial t} \Delta \rho + \Delta(\rho v) = -V_S \Delta \rho + \Delta(\rho v) = 0 \quad (11)$$

where V_S is the shock speed. This relation is the hydrodynamic shock condition. To generalize it beyond 1D, it suffices to take $\mathbf{v} \cdot \mathbf{n}$ instead of v where \mathbf{n} is the unit normal vector on the shock wave front pointing towards the region with lower pressure. It looks as follows

$$-V_S \Delta(\rho v) + \Delta(\rho \mathbf{v} \cdot \mathbf{n}) = 0 . \quad (12)$$

The minus sign in front of V_S is merely a matter of orientation. In eq. (11) the orientation is along the positive x-axis. In eq. (12) it is along the unit vector \mathbf{n} . This is the first of the three *Rankine–Hugoniot* relations. The other two can analogously be derived from the Eulerian form of momentum and energy equations in eq. (1). The three Rankine–Hugoniot conditions are

$$\begin{aligned} V_S \Delta \rho &= \mathbf{n} \cdot \Delta(\rho \mathbf{v}) \\ V_S \Delta(\rho \mathbf{v}) &= \mathbf{n} \cdot \Delta(\rho \mathbf{v} \mathbf{v} + p \mathbb{I}) \\ V_S \Delta E_t &= \mathbf{n} \cdot \Delta\left(\rho \left(e + \frac{v^2}{2} + \frac{p}{\rho}\right) \mathbf{v}\right) \end{aligned} \quad (13)$$

Now, for the purposes of this report we would like to write a shock condition in terms of the shock speed as a function of the initial conditions p_0, ρ_0, v_0 and the final pressure p_1 as pressure is the variable on which we shall be focusing in the simulation data results. Consider a pressure discontinuity $\Delta p = p_1 - p_0$. Use the 1D mass and momentum equations to obtain that

$$V_S^2 = \frac{\Delta \rho v^2 + p}{\Delta \rho} \quad (14)$$

Assume that $v_0 = 0$. This assumption may not seem entirely reasonable, but is very helpful in simplifying the problem and will be correct for most of our purposes. Furthermore, we shall see that it can be easily removed when we wish. Combining eq. (14) with the shock conditions derived from the Energy equation, this then results in

$$V_S^2 = v_s^2 + \frac{\gamma + 1}{2\rho_0} \Delta p \quad (15)$$

where $v_s = \sqrt{\frac{\gamma p_0}{\rho}}$ is the speed of sound under the initial conditions. Notice that for $\Delta p = 0$ this expression gives $V_S = v_s$ as we should expect.

In case we cannot assume $v_0 = 0$ (and do not wish to view the problem from a moving reference frame) the expression changes only slightly.

$$\begin{aligned}
(V_S - v_0)^2 &= v_s^2 + \frac{\gamma + 1}{2\rho_0} \Delta p \\
V_S &= v_0 + \sqrt{v_s^2 + \frac{\gamma + 1}{2\rho_0} \Delta p}
\end{aligned} \tag{16}$$

Of course, for the 3D case, one simply writes

$$V_S = \mathbf{n} \cdot \mathbf{v}_0 + \sqrt{v_s^2 + \frac{\gamma + 1}{2\rho_0} \Delta p} \tag{17}$$

Derivation of MHD equation, discussion of the integration scheme used

Test informatievaardigheden!!!

2.4 Magnetohydrodynamic fluid equations

Since the aim of this bachelor project is mainly using simulation software to get an understanding of the behaviour of waves in plasma and the subject of magnetohydrodynamics is a really complex one, we will merely state the results relevant as theoretical background for our simulations and skim over the derivations, without diving into every technical detail. Where necessary, the assumptions behind the equations and how these assumptions limit the applicability is discussed. We provide references to the material where we found the relevant formulas and derivations can often be found.

There are two approaches commonly taken in the literature to derive the MHD equations. They are either derived from kinetic gas theory, or postulated with added justification of why they can accurately describe plasmas.

We will now sketch the first approach in order to get some insight in the underlying assumptions of the theory. A plasma is an ionised gas consisting of positive and negative ions. In the case of the corona of the sun this is mainly ionised hydrogen. Therefore the negative ions are free electrons and the positive ions protons, which are a lot heavier than electrons. When the characteristic timescales τ_e and τ_i between two collisions of electrons, respectively ions, is much shorter than characteristic timescales τ_f at which macroscopic variables change we can use a fluid description. At these timescales the individual interactions of individual particles are not relevant anymore.

The plasma can then be described as two different fluids, commonly referred to as the *two-fluid theory*. The electron gas is one fluid and the proton gas the other. The next assumption that is made, is that the relaxation time τ_T until the electron fluid and ion fluid are in thermal equilibrium after a slight disturbance is also a lot smaller than τ_f . Finally, we assume that the fluid has no net charge. Not globally, but also not locally. This means that in every large enough volume, for every ion with charge Z , there are also about Z electrons in this volume. When all this applies, the variables describing the different fluids can be averaged or added together, to describe the plasma as one fluid.

add reference to cursus Poedts and course notes arxiv

The MHD equations can then be found by adding the Maxwell equations to the HD equations. There is one complication: the HD equations are invariant under Galilean transformations. However the Maxwell equations are invariant under Lorentz transformations, so we cannot simply add them to the HD equations and expect a consistent picture. To solve this the term for the displacement current $\epsilon_0 \frac{\partial \mathbf{E}}{\partial t}$ is dropped which results in a set of equations that are invariant under Galilean transformations.

referentie

Understanding the averaging process which brings us from two-fluid theory to the description given by the magnetohydrodynamic equations is important for understanding what the plasma variables actually represent and when this representation is an accurate depiction of the state of the plasma. Denote with n_α the number density of a certain type of particle, m_α the mass of one particle, \mathbf{u}_α

the velocity of a fluid element of the fluid consisting from particles α and with p_α the pressure of the gas of these particles. Let the subscript e denote variables concerning the electrongas and i variables describing the iongas. The variables describing the plasma are the following linear combinations of variables describing the electron and ion gas:

$$\begin{aligned}\rho &= n_e m_e + n_i m_i \\ \mathbf{v} &= (n_e m_e \mathbf{u}_e + n_i m_i \mathbf{u}_i) / \rho \\ \mathbf{J} &= -e(n_e \mathbf{u}_e - Z n_i \mathbf{u}_i) \\ p &= p_e + p_i\end{aligned}\quad (18)$$

Where e is the charge of an electron and Z the charge of an ion as a multiple of the electron charge. The first equation is the *total mass density*, the second the *center of mass velocity*, the third the *current density* and the last one describes the *total pressure*.

Finally, the viscosity and heat flow are neglected like in the HD case. Furthermore, for the ideal MHD case the resistivity of the fluid is neglected. The extra equations we need are then:

$$\begin{aligned}\frac{\partial \mathbf{B}}{\partial t} &= -\nabla \times \mathbf{E} \\ \nabla \cdot \mathbf{B} &= 0 \\ \nabla \times \mathbf{B} &= \mu_0 \mathbf{J}\end{aligned}$$

We do not need an equation relating the charge distribution to the electric field in the first equation since we assumed the fluid is locally neutral. Furthermore the displacement term in the third equation was neglected.

Adding everything together such as in [REFERENCE TO ONE OF THE COURSES] yields the ideal MHD equations:

reference to
course notes
poedts

$$\begin{aligned}\frac{\partial \rho}{\partial t} + \nabla \cdot (\rho \mathbf{v}) &= 0 \\ \rho \left(\frac{\partial \mathbf{v}}{\partial t} + \mathbf{v} \cdot \nabla \mathbf{v} \right) + \nabla p - \mathbf{J} \times \mathbf{B} &= 0 \\ \frac{\partial p}{\partial t} + \mathbf{v} \cdot \nabla p + \gamma p \nabla \cdot \mathbf{v} &= 0 \\ \frac{\partial \mathbf{B}}{\partial t} - \nabla \times (\mathbf{v} \times \mathbf{B}) &= 0\end{aligned}\quad (19)$$

Where

$$\mathbf{J} = \frac{\nabla \times \mathbf{B}}{\mu_0}.$$

We need one additional equation which the initial condition has to satisfy:

$$\nabla \cdot \mathbf{B} = 0$$

which expresses that there are no magnetic monopoles. By acting with $\nabla \cdot$ on the fourth equation in eq. (19) we see that if the initial equation satisfies $\nabla \cdot \mathbf{B} = 0$, it is automatically satisfied for all later times:

$$\frac{\partial (\nabla \cdot \mathbf{B})}{\partial t} = 0$$

The equations used by PLUTO in the ideal case have a slightly different form:

reference to
user guide

$$\begin{aligned}
& \frac{\partial \rho}{\partial t} + \nabla \cdot (\mathbf{m}) = 0 \\
& \frac{\partial \mathbf{m}}{\partial t} + \nabla \cdot \left[\mathbf{m}\mathbf{v} - \mathbf{B}\mathbf{B} + I \left(p + \frac{B^2}{2} \right) \right]^T = -\rho \nabla \Phi + \rho \mathbf{g} \\
& \frac{\partial \mathbf{B}}{\partial t} + \nabla \times (c\mathbf{E}) = 0 \\
& \frac{\partial (E_t + \rho \Phi)}{\partial t} + \nabla \cdot [(E_t + p_t + \rho \Phi) \mathbf{v} - \mathbf{B}(\mathbf{v} \cdot \mathbf{B})] = \mathbf{m} \cdot \mathbf{g}
\end{aligned} \tag{20}$$

where, as with the HD equations, $\mathbf{m} = \rho \mathbf{v}$ and E_t is again the total energy density, this time with an extra term for the magnetic field:

$$E_t = \rho e + \frac{\rho v^2 + B^2}{2}$$

$c\mathbf{E}$ is given by:

$$c\mathbf{E} = -\mathbf{v} \times \mathbf{B}$$

note that the equations do not formally depend on the speed of light, but it is kept in the equations for consistency with the relativistic case.

2.5 Magnetohydrodynamic waves

For the discussion of linear magnetohydrodynamic waves we take an initial condition with homogeneous plasma in equilibrium. Denote with ρ_0 , p_0 , \mathbf{v}_0 and \mathbf{B}_0 these equilibrium values. To derive the equations for the waves, consider slight perturbations ρ_1 , p_1 , \mathbf{v}_1 and \mathbf{B}_1 of this equilibrium state, just like what was done to find the HD waves.

Firstly, rewrite the basic MHD equations into a form which is easier to linearize, this means that we shall remove the cross products in the original equations as follows:

$$\begin{aligned}
-\mathbf{J} \times \mathbf{B} &= -(\nabla \times \mathbf{B}) \times \mathbf{B} = (\nabla \mathbf{B}) \cdot \mathbf{B} - \mathbf{B} \cdot \nabla \mathbf{B} \\
\nabla \times \mathbf{E} &= -\nabla \times (\mathbf{v} \times \mathbf{B}) = \mathbf{B} \nabla \cdot \mathbf{v} + \mathbf{v} \cdot \nabla \mathbf{B} - \mathbf{B} \cdot \nabla \mathbf{v}
\end{aligned} \tag{21}$$

The MHD equations now become

$$\begin{aligned}
& \frac{\partial \rho}{\partial t} + \nabla \cdot (\rho \mathbf{v}) = 0 \\
& \rho \frac{\partial \mathbf{v}}{\partial t} + \rho \mathbf{v} \cdot \nabla \mathbf{v} + (\gamma - 1) \nabla(\rho e) + (\nabla \mathbf{B}) \cdot \mathbf{B} - \mathbf{B} \cdot \nabla \mathbf{B} = 0 \\
& \frac{\partial e}{\partial t} + \mathbf{v} \cdot \nabla e + (\gamma - 1) e \nabla \cdot \mathbf{v} = 0 \\
& \frac{\partial \mathbf{B}}{\partial t} + \mathbf{v} \cdot \nabla \mathbf{B} + \mathbf{B} \nabla \cdot \mathbf{v} - \mathbf{B} \cdot \nabla \mathbf{v} = 0
\end{aligned} \tag{22}$$

Of course the condition that $\nabla \cdot \mathbf{B} = 0$ remains. In this form the equations are much easier to linearize:

$$\begin{aligned}
& \frac{\partial \rho_1}{\partial t} + \nabla \cdot (\rho_0 \mathbf{v}_1) = 0 \\
& \rho_0 \frac{\partial \mathbf{v}_1}{\partial t} + (\gamma - 1) \nabla(\rho_1 e_0) + \nabla(\rho_0 e_1) + (\nabla \mathbf{B}_1) \cdot \mathbf{B}_0 - \mathbf{B}_0 \cdot \nabla \mathbf{B}_1 = 0 \\
& \frac{\partial e_1}{\partial t} + (\gamma - 1) e_0 \nabla \cdot \mathbf{v}_1 = 0 \\
& \frac{\partial \mathbf{B}_1}{\partial t} + \mathbf{B}_0 \nabla \cdot \mathbf{v}_1 - \mathbf{B}_0 \cdot \nabla \mathbf{v}_1 = 0
\end{aligned} \tag{23}$$

The second one of these equations eq. (23) is the linearized momentum equation. We shall work from this one as it lends itself the most for our discussion of ideal MHD waves, because it directly describes flow velocity. Plugging the other three into this equation gives us the essential equation for ideal MHD waves:

$$\frac{\partial^2 \mathbf{v}_1}{\partial t^2} = \left((\mathbf{v}_a \nabla)^2 \mathbb{I} + (v_a^2 + v_s^2) \nabla \nabla - \mathbf{v}_a \cdot \nabla (\nabla \mathbf{v}_a + \mathbf{v}_a \nabla) \right) \cdot \mathbf{v}_1 \tag{24}$$

where

$$v_s = \sqrt{\frac{\gamma p_0}{\rho_0}} \tag{25}$$

and

$$\mathbf{v}_a = \frac{\mathbf{B}_0}{\sqrt{\rho_0}}. \tag{26}$$

We introduce the constants v_s and \mathbf{v}_a as they will be the wave velocities of the solutions of the wave equation eq. (24). The constant v_s is the acoustic speed known from regular hydrodynamics. The constant \mathbf{v}_a is known as the *Alfvén* velocity and it is a vector in the same direction as the background magnetic field \mathbf{B}_0 .

Notice that if we set $\mathbf{B} = 0$ eq. (24) becomes

$$\frac{\partial^2 \mathbf{v}_1}{\partial t^2} = v_s^2 \nabla^2 \mathbf{v}_1$$

which is exactly what we would expect as this is wave equation in the normal hydrodynamic case. This is an important sanity check for our method.

Next we seek sinusoidal wave solutions. For now we shall also limit the discussion the waves in the velocity vector field as the waves in the scalar pressure and density fields and the magnetic vector field can easily be expressed in terms of the velocity field using eq. (23). The solutions we look for are of the form

$$\mathbf{v}_1 = \bar{\mathbf{v}} \exp(i(\omega t - \mathbf{k} \cdot \mathbf{x})) .$$

Under the constraint of having to provide sinusoidal wave solutions eq. (24) becomes

$$[(\omega^2 - (\mathbf{k} \cdot \mathbf{b})^2) \mathbb{I} - (b^2 + c^2) \mathbf{k} \mathbf{k} + \mathbf{k} \cdot \mathbf{b} (\mathbf{k} \mathbf{b} + \mathbf{b} \mathbf{k})] \cdot \bar{\mathbf{v}} = 0 . \tag{27}$$

Without any loss of generality we may assume that $\mathbf{v}_a = (v_a, 0, 0)$ and $\mathbf{k} = (k_x, k_y, 0) = (k \cos \theta, k \sin \theta, 0)$ where θ is the angle between \mathbf{v}_a and \mathbf{k} . Filling in these into eq. (27) results in

$$\begin{pmatrix} \omega^2 - k_x^2 v_s^2 & -k_y k_x v_s^2 & 0 \\ -k_y k_x v_s^2 & \omega^2 - k_y^2 (v_a^2 + v_s^2) - k_x^2 v_a^2 & 0 \\ 0 & 0 & \omega^2 - k_x^2 v_a^2 \end{pmatrix} \begin{pmatrix} \bar{v}_x \\ \bar{v}_y \\ \bar{v}_z \end{pmatrix} = \begin{pmatrix} 0 \\ 0 \\ 0 \end{pmatrix} \quad (28)$$

This has a non-trivial solution when the determinant of the matrix in eq. (28) is 0. This results in the dispersion relation

$$(\omega^2 - k^2 v_a^2 \cos^2 \theta) (\omega^4 - \omega^2 k^2 (v_a^2 + v_s^2) + v_a^2 v_s^2 k^4 \cos^2 \theta) = 0. \quad (29)$$

We shall first discuss the factor $(\omega^4 - \omega^2 k^2 (v_a^2 + v_s^2) + v_a^2 v_s^2 k^4 \cos^2 \theta)$ of which the roots are

$$\omega_{\pm}^2 = \frac{k^2}{2} \left[v_a^2 + v_s^2 \pm \sqrt{(v_a^2 + v_s^2)^2 - 4v_a^2 v_s^2 \cos^2 \theta} \right] \quad (30)$$

These solutions correspond to the so-called fast (+) and slow (-) magnetosonic waves. Notice that because $(v_a^2 + v_s^2)^2 - 4v_a^2 v_s^2 \cos^2 \theta \geq (v_a^2 - v_s^2)^2 \geq 0$ the square root can always be taken. One can readily see that they are the result of a quite complicated interplay between the hydrodynamic and magnetic sides of the story. We will rely on the simulations to get a better understanding of their behaviour.

The only root of the first factor in eq. (29) is $\omega^2 = k_x^2 b^2$. This solution is of great interest as it does not contain the same complicated magnetosonic interaction and solely depends on the nature of the magnetic field. The density irregularities only provide the wave's momentum. The restoring force is entirely generated by the tension in the magnetic field.

The wave corresponding to $\omega_A^2 = k_x^2 b^2$ is called the *Alfvén* wave. Notice that its direction corresponds to that of the magnetic field, where $\omega_A = k_x b$ lies in the same direction and $-\omega_A$ in the opposite direction. It should be noted that this solution is non-relativistic. As the magnetic field becomes stronger in comparison to the density the Alfvén wave becomes a regular electromagnetic wave.

Now, the first roots we had - the magnetosonic waves - are combinations of Alfvén waves and ordinary sound waves. There are two types because the Alfvén and sound waves can either be in phase or in antiphase to one another. In the first case ω_+ the region of high pressure will correspond to a high magnetic field density, which causes the resulting wave to be driven forward by both ordinary hydrodynamic pressure and the tension of the concentrated magnetic field lines. In the other case ω_- these same two forces work against each other, slowing the wave.

2.5.1 Group speed

The wave speed that is derived from the simulations is the group speed and not the phase speed of the waves. We use the relation eq. (9) to calculate this quantity. For the Alfvén waves, this is easy and yields:

$$\mathbf{v}_{ga} = \hat{\mathbf{k}} \cos \theta v_a \quad (31)$$

Where θ is again the angle between $\hat{\mathbf{k}}$ and the magnetic field \mathbf{B} .

For the slow and fast magnetosonic waves, this is a lot more involved. A derivation can be found in [REF]. The result is $(v_{\pm} = \omega_{\pm}/k)$:

$$\mathbf{v}_{\pm} = \frac{v_{\pm}^4(\theta) \hat{\mathbf{k}} - v_s^2 v_a^2 \hat{\mathbf{B}} \cos \theta}{v_{\pm}(\theta) [2v_{\pm}^2 - (v_s^2 + v_a^2)]} \quad (32)$$

This gives the group speed of the fast and slow magnetosonic modes as a function of the angle θ between the wave vector \mathbf{k} and the magnetic field \mathbf{B} . In fig. 1 this relation is plotted in polar form for a few different values of the plasma- β . The β used here is one calculated using the dimensionless

ref to course
notes for just-
ification of these
claims

ref naar http://www.ss.ncu.edu.tw/~lyu/lecture_files_en/lyu_SPP_Book_A4format_pdf.html/pdf_1_Ch/lyu_SPP_Chapter_6.pdf

units introduced in section 2.6. A derivation to get from the value of β to values for v_a and v_s needed to calculate the group velocity can be found in that section as well. We remark that the group speed of the slow-mode along the magnetic field has a maximum speed equal to $\min\{v_a, v_s\}$ and the speed of the fast mode is $\max\{v_a, v_s\}$ along the x -axis.

Group speed of MHD waves for different values of β

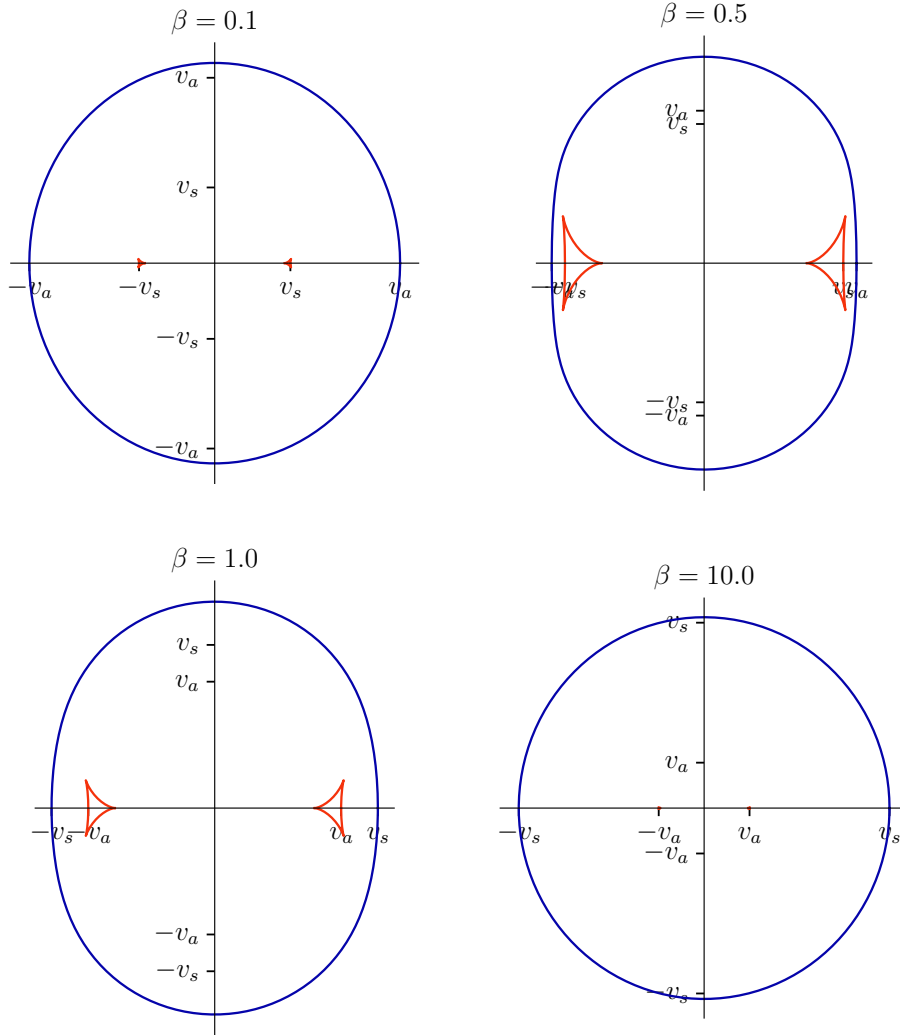


Figure 1: Group speed diagrams for the fast (blue) and slow (red) magnetosonic waves. The magnetic field points along the x -axis. The magnetic field is oriented along the horizontal axis. The lines represent the group speed of the wave (distance from origin) as a function of the angle θ between the wave vector \mathbf{k} and magnetic field \mathbf{B} .

Magnetohydrodynamic shocks

To derive the Rankine–Hugoniot conditions for MHD shocks, one simply uses eq. (19) as it is already in its Eulerian form and preforms the same calculations as for the Rankine–Hugoniot conditions for HD shocks. This yields:

$$\begin{aligned}
 V_S \Delta \rho &= \mathbf{n} \cdot \Delta(\rho \mathbf{v}) \\
 V_S \Delta(\rho \mathbf{v}) &= \mathbf{n} \cdot \Delta(\rho \mathbf{v} \mathbf{v} + (p + \frac{B^2}{2}) \mathbb{I} - \mathbf{B}\mathbf{B}) \\
 V_S \Delta E_t &= \mathbf{n} \cdot \Delta((\rho \frac{v^2}{2} + \frac{\gamma}{\gamma-1} p + B^2) \mathbf{v} - \mathbf{v} \cdot \mathbf{B}\mathbf{B}) \\
 V_S \Delta \mathbf{B} &= \mathbf{n} \cdot \Delta(\mathbf{v}\mathbf{B} - \mathbf{B}\mathbf{v})
 \end{aligned} \tag{33}$$

2.6 Units

The PLUTO code works, in general, with dimensionless code-units. This is done by defining a unit density ρ_0 , unit velocity v_0 and unit length L_0 . From these, unit time can be defined as $t_0 = L_0/v_0$. Inspired by eq. (25) and eq. (26) we defin $p_0 = \rho_0 v_0^2$ and $B_0 = v_0 \sqrt{4\pi\rho_0}$. Next, we use the substitutions $v_0 \mathbf{v}_u = \mathbf{v}$, $\rho_0 \rho_u = \rho$, $L_0 \mathbf{x}_u = \mathbf{x}$, $t_0 t_u = t$, $p_0 p_u = p$ and $B_0 \mathbf{b}_u = \mathbf{B}$ in eq. (19). Here the subscript u denotes that these numbers or vectors are dimensionless, the units are contained in the factors with subscript 0.

$$\begin{aligned}
 \frac{\rho_0 v_0^2}{L_0} \rho_u \left(\frac{\partial \mathbf{v}_u}{\partial t_u} + \mathbf{v}_u \cdot \nabla_u \mathbf{v}_u \right) + \frac{\rho_0 v_0^2}{L_0} \nabla_u p_u - \frac{\rho_0 v_0^2}{L_0} \frac{\nabla_u \times \mathbf{B}_u}{\mu_0} \times \mathbf{B}_u &= 0 \\
 \frac{p_0 v_0}{L_0} \frac{\partial p_u}{\partial t_u} + \frac{p_0 v_0}{L_0} \mathbf{v}_u \cdot \nabla_u p_u + \frac{p_0 v_0}{L_0} \gamma p_u \nabla_u \cdot \mathbf{v}_u &= 0 \\
 \frac{B_0 v_0}{L_0} \frac{\partial \mathbf{B}_u}{\partial t_u} - \frac{B_0 v_0}{L_0} \nabla_u \times (\mathbf{v}_u \times \mathbf{B}_u) &= 0
 \end{aligned} \tag{34}$$

We see that all the units drop out of the equations and we are left with a set of dimensionless equations. This highlights an important fact for ideal MHD: the equations are scale-invariant. For the behaviour of waves the absolute scales are not important, but only the relative magnitude of the characteristic scales for a wave. When we have a wave with wavelength λ_1 and frequency f_1 , it will show the same behaviour as a wave with wavelength λ_2 and frequency f_1/λ_1 in the same medium (that is, same Alfvén speed).

Because the ideal MHD equations are in fact dimensionless (without sources), we can carry out the simulations in dimensionless units and later scale our results to match conditions as found in e.g. the solar corona, under the condition that the relative magnitudes of ρ_0 , v_0 and L_0 are correct.

the plasma- β in these dimensionless units is defined as

$$\beta = \frac{p}{B^2/2} \tag{35}$$

We find that

$$v_a = \frac{B_0}{\sqrt{\rho_0}} = \sqrt{\frac{p_0}{2\beta\rho_0}} = \sqrt{\frac{1}{2\beta}} v_0 \tag{36}$$

and that

$$v_s = \sqrt{\gamma \frac{p_0}{\rho_0}} = \sqrt{\gamma} v_0 \tag{37}$$

These expressions will be necessary to compare the simulation data to the theoretical results from the previous sections.

3 Modeling shock waves

quickfix As a testcase to learn how to use the PLUTO software we simulated hydrodynamic and magnetohydrodynamic blastwaves in a 2D domain. The initial condition for the simulations is a circle with radius 0.3 (in code units) with higher pressure. The pressure outside the circle is 1, in code units. For the pressure inside the circle two scenarios were simulated. One with a large pressure difference, where the pressure inside the circle is 5. In the other scenario a lower pressure difference was used: the pressure inside the circle was 1.5. The reason for using different pressure differences is to see the non-linear effects in the shock-wave with high pressure difference.

3.1 Hydrodynamic shockwave

First some technical details of the simulation (all physical quantities are in code units). The simulation was done on a 1024×1024 grid for a period of $t = 1.5$ with an initial time step of $1e - 4$. A snapshot of the variables describing the system was saved every 0.03 time units, for a total of 50 snapshots (excluding the initial condition). The Pluto simulation used 996 steps.

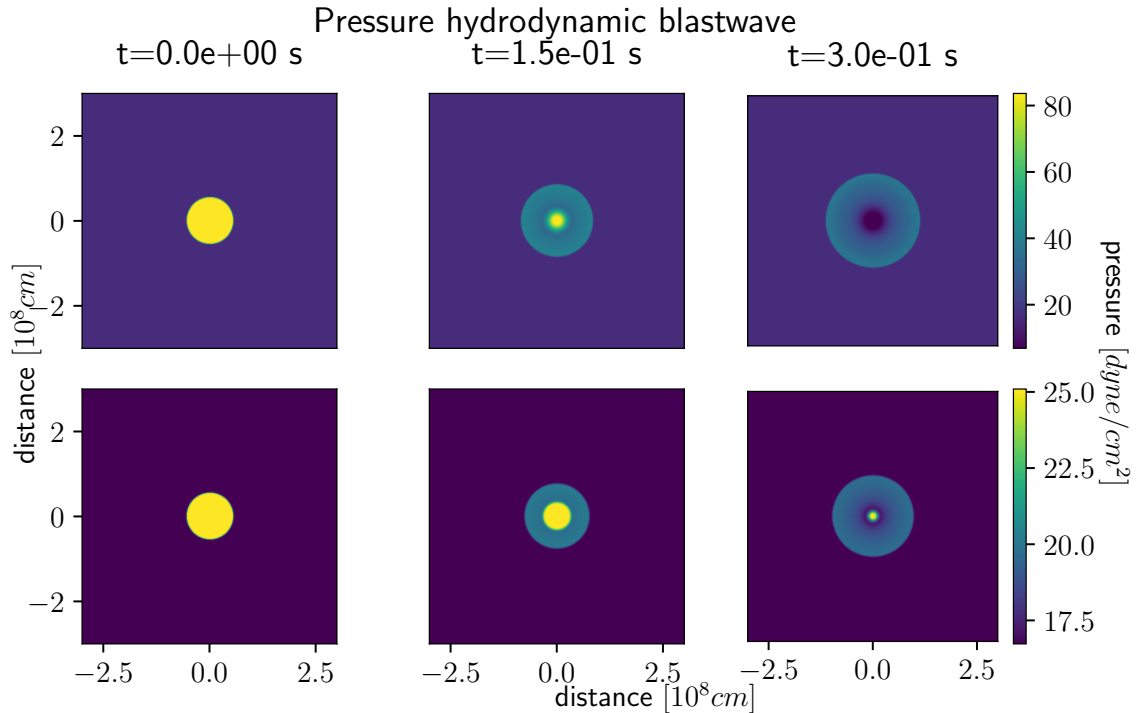


Figure 2: Pressure profile for a blastwave in an ideal fluid at different times. The top row start with the larger pressure difference of 5/1, the bottom row is the blastwave with smaller pressure difference of 1.5/1.

In fig. 2 the pressureprofile of both scenarios is plot for the initial condition and two frames right after the start of the simulation. In fig. 3 the profile is plotted for later times. Its imedeatly clear that the shock wave with the higher pressure difference travels faster then the other one, but the general shape of the wave is the same.

In fig. 4 the speed of the wave front along the positive x -axis is plotted as a function of time, and this confirms that the wave speed is lower with a lower pressure difference. The group speed was calculated in two ways. The first was to start at a point at the edge of the domain and find the first point on the line from this point to the center with a pressure higher than 1.01 times the background pressure. This gives a relation $x(t)$ for the position of the wave-front along this line. The speed was

calculated using numerical differentiation with the following central difference:

$$f'(t_0) = \frac{f(t+dt) - f(t-dt)}{2dt} + O(dt^2)$$

found in [REF]. This is the simulated speed, represented by the dots.

Using [FORMULA SHOCK SPEED RIEMANN PROBLEM] the theoretical speed of a shock in a Riemann problem was calculated using the highest pressure in the domain as max pressure and 1 as the low pressure. This is plotted as the line.

Firstly, we notice that the speeds calculated with the first method tend to lie on some lines. This is a numerical from the discretization of time and space. It has nothing to do with the physics of the problem. The slight deviations from this lines are because PLUTO does not use fixed time steps for integration, therefore the time between two snapshots is not always exactly the same.

reference
naar cursus
numerieke
wiskunde

calculate shock
speed in a Rie-
mann problem
as function of
the two pres-
sures

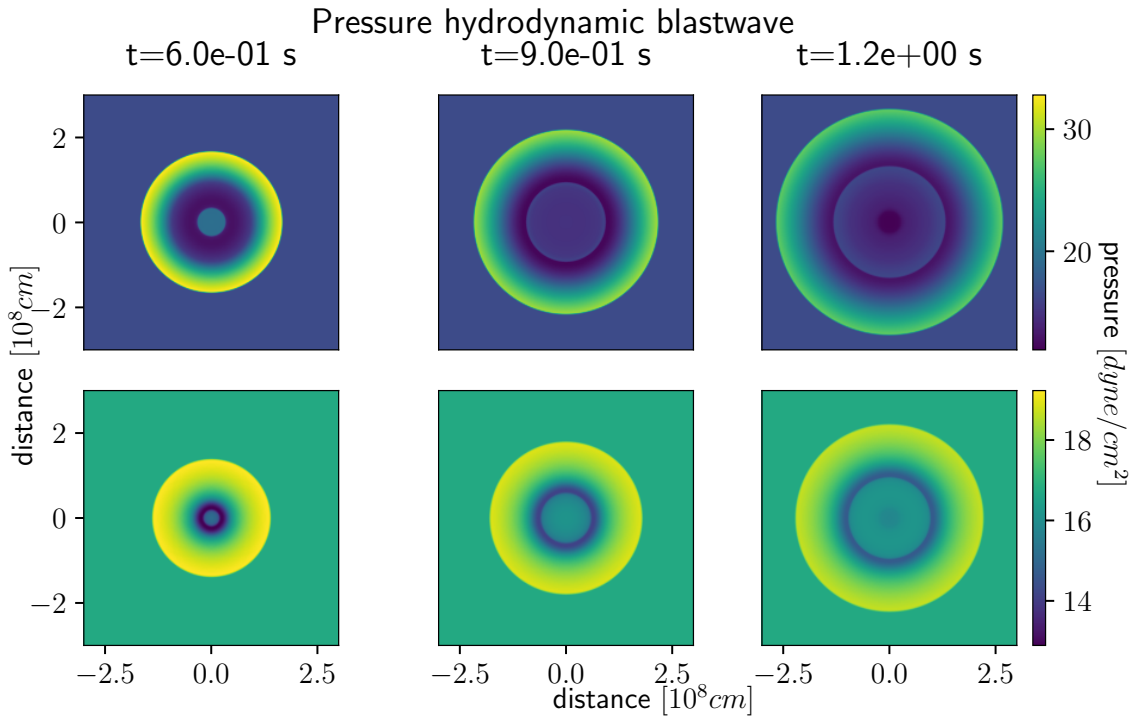


Figure 3: Pressure profile for a blastwave in an ideal fluid at larger timescales. Initial conditions for each row are the same as in fig. 2.

We see that the curve closely follows the dots with the lower pressure difference, whereas this is not the case for the higher pressure difference. There are two main reasons for this discrepancy. Firstly, this is not exactly the same as a Riemann problem, certainly at a later stage when the sharp boundary has smoothed out. Secondly, due to non-linear effects we cannot assume that the wave is non-dispersive. This means that the first edge of the wave is probably traveling faster than the group speed of the center of this shockwave, which is the value calculated in the Riemann problem. These two effects together can explain the difference in speed between the value for a Riemann problem and the value calculated from the simulation data.

We remark that approximating the shock as a Riemann problem is a crude first-order approximation. The PLUTO code calculates flow velocities like this in every integration step. This small example highlights the importance of robust integrators and Riemann solvers, together with small enough time steps, to accurately model flow variables in the vicinity of large gradients.

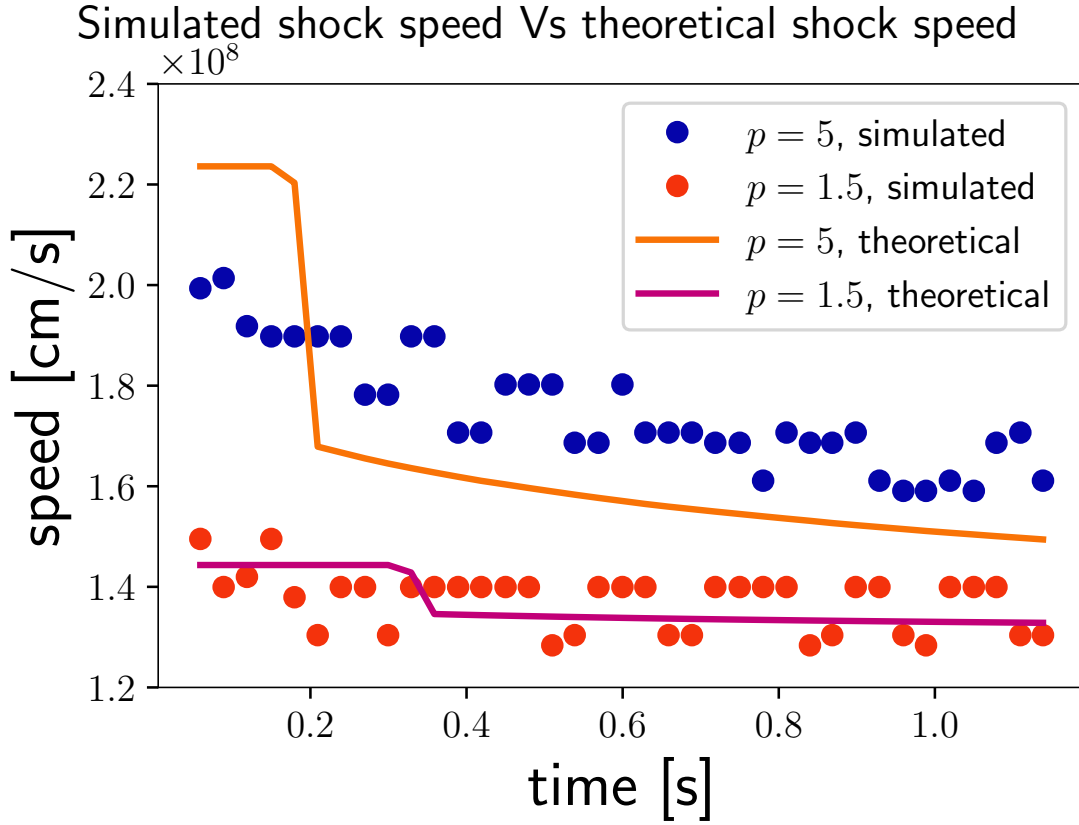


Figure 4: the speed of the wave as a function of time, along the x -axis. The dots represent the speed calculated from the simulation data by deriving the function $x(t)$ that represents the position of the wave front. The lines represent the theoretical shock speed in a Riemann-problem with as high pressure the highest pressure in the domain, and low pressure 1.

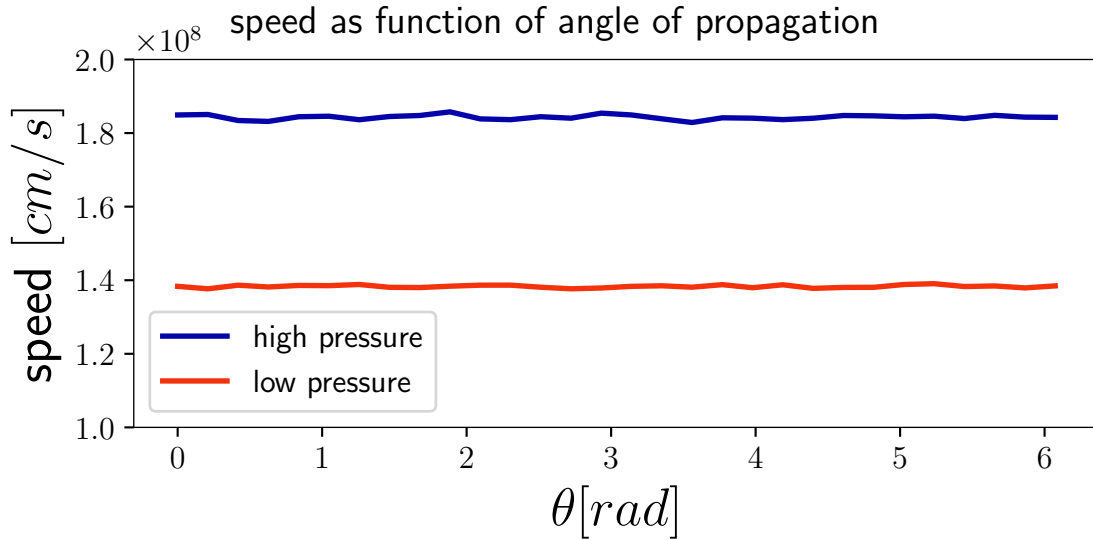


Figure 5: The wave speed as a function of the angle between the x -axis and the line connecting a point on the wave-front with the center of the domain. The wavespeed is calculated from the simulation data.

Finally fig. 5 shows that the wave is isotropic. The speed of the wavefront along lines making an

angle θ with the x -axis through the origin was calculated. The slight variations in speed are again artifacts of the space discretization.

3.2 Magnetohydrodynamic shock wave

In the magnetohydrodynamic case the same initial conditions were used, but a uniform magnetic field in the x -direction was added. The simulation was done for varying strengths of the magnetic field. In fig. 6 a snapshot of the blast wave after 1 unit of time is plotted for different values of β .

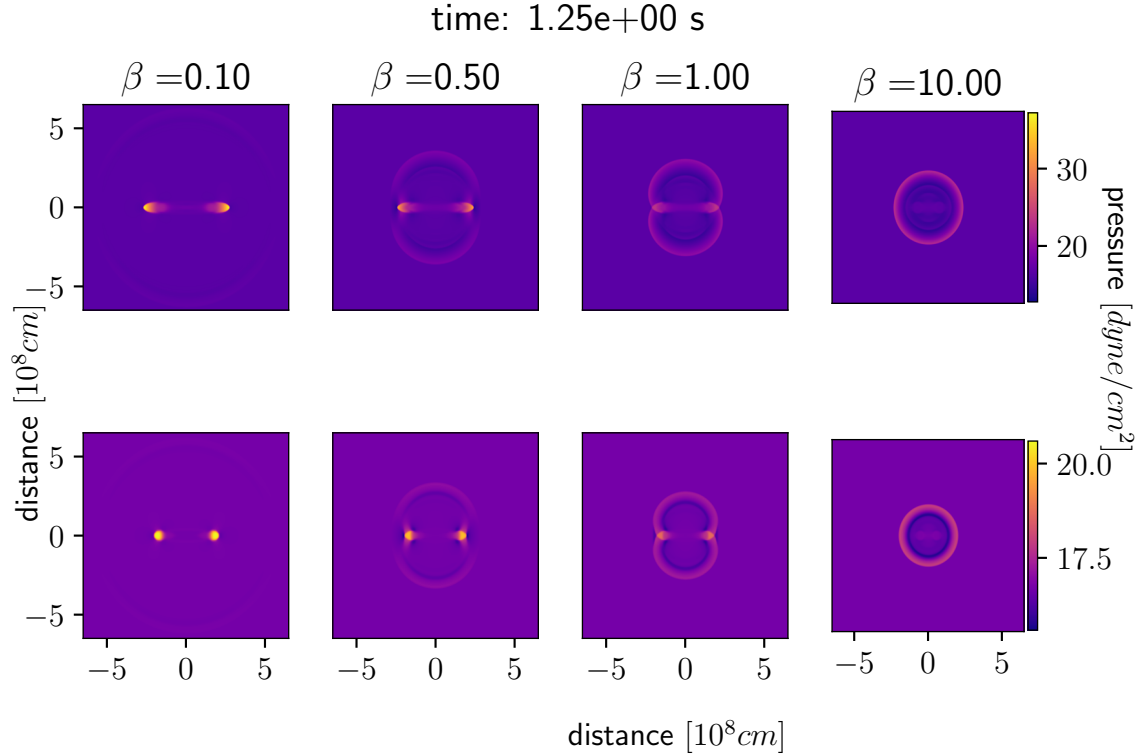


Figure 6: Plots of the pressure of an MHD blastwave with the same initial conditions as in fig. 2: high pressure difference for the top row, lower for the bottom row.

in the plots with $\beta \in \{0.5, 1\}$ there is a clear distinction between a fast shock wave spreading in all directions, and two small waves following the magnetic field. In the plot with $\beta = 0.1$ this fast wave is barely visible nearing the edge of the domain, but the two small waves stand out from the uniform background. for $\beta = 1$ the fast wave is almost perfectly spherical and very visible, while the two smaller waves are very faint. We observe that if the magnetic field gets stronger, the wave becomes faster and most of the energy gets concentrated in the slow-mode, while the fast mode gets less energetic. To go a bit more in-depth we plot the diagram depicting the group speeds over the simulation data and see how well they match. This can be seen in fig. 7 and fig. 8.

calculate this flux?

Since the initial condition is not a delta function, the wave will not nicely lie on the diagram of the group speed. We have to correct for the finite radius of the circle with higher pressure in the initial condition. By adding this circle to the diagram of the group speed, where the relevant speeds v_a , v_s to calculate the group speed are found using eq. (36) and eq. (37), the dashed lines are found. These dashed lines do form an accurate boundary of the waves. However for the fast wave mode we can make the same remark as in the hydrodynamic case: namely that the wave is faster than the linear wave in a medium with pressure p_0 due to the shock at the start.

We also see again that the wave is faster with a high pressure difference. Due to the difficulty of accurately detecting the waves in the simulation data, either because they are really faint with small

or large β , or there is a lot of interference between the modes when $\beta \sim 1$, no accurate calculations of the wave speed from the simulation data could be made.

The effects of the magnetic field are clear, removing the isotropy of the wave and introducing two strong wave modes following the magnetic field in opposite directions. When the magnetic field becomes small, a quick comparison shows that the wave speed goes to the wave speed of an HD-wave as expected.

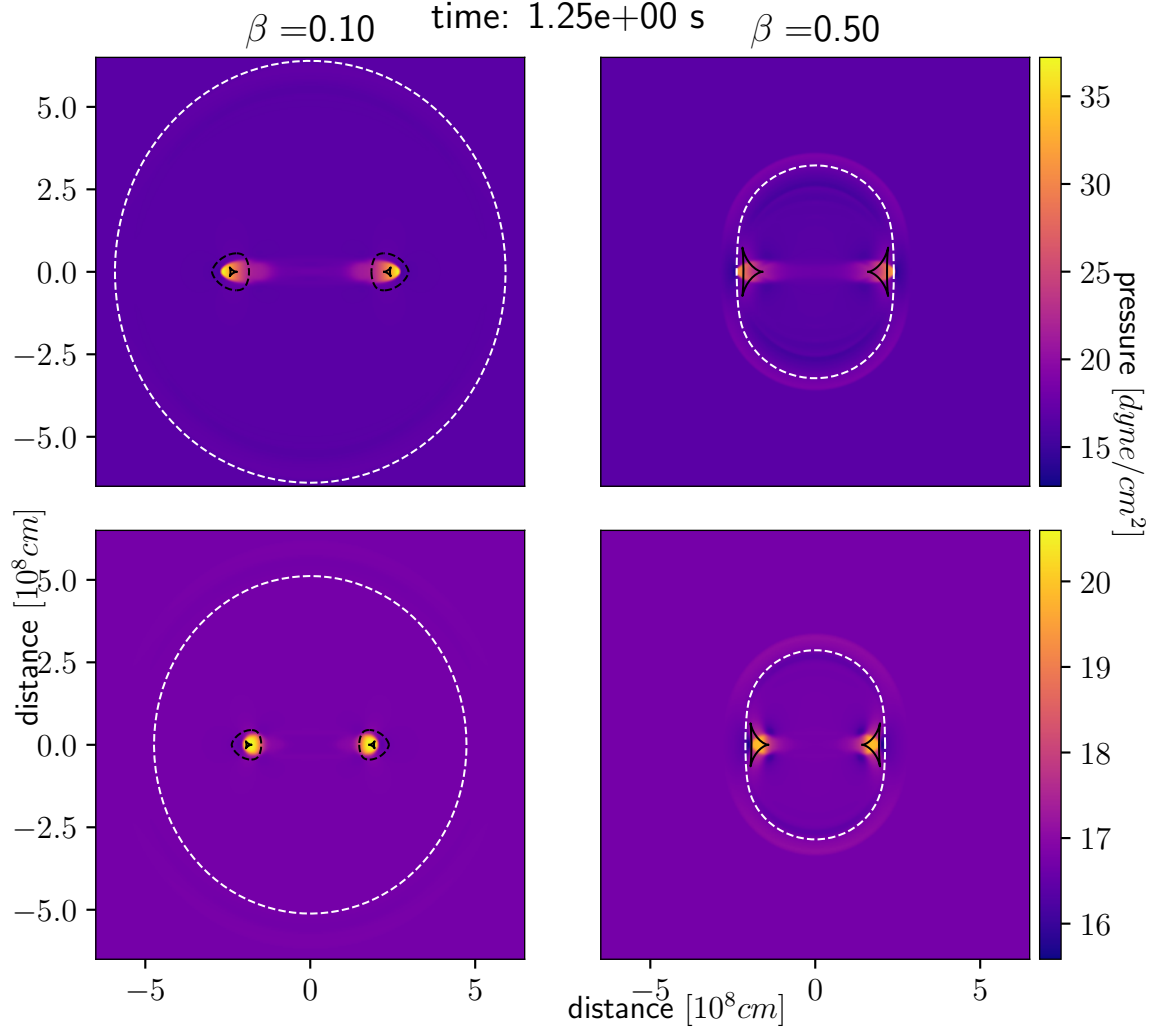
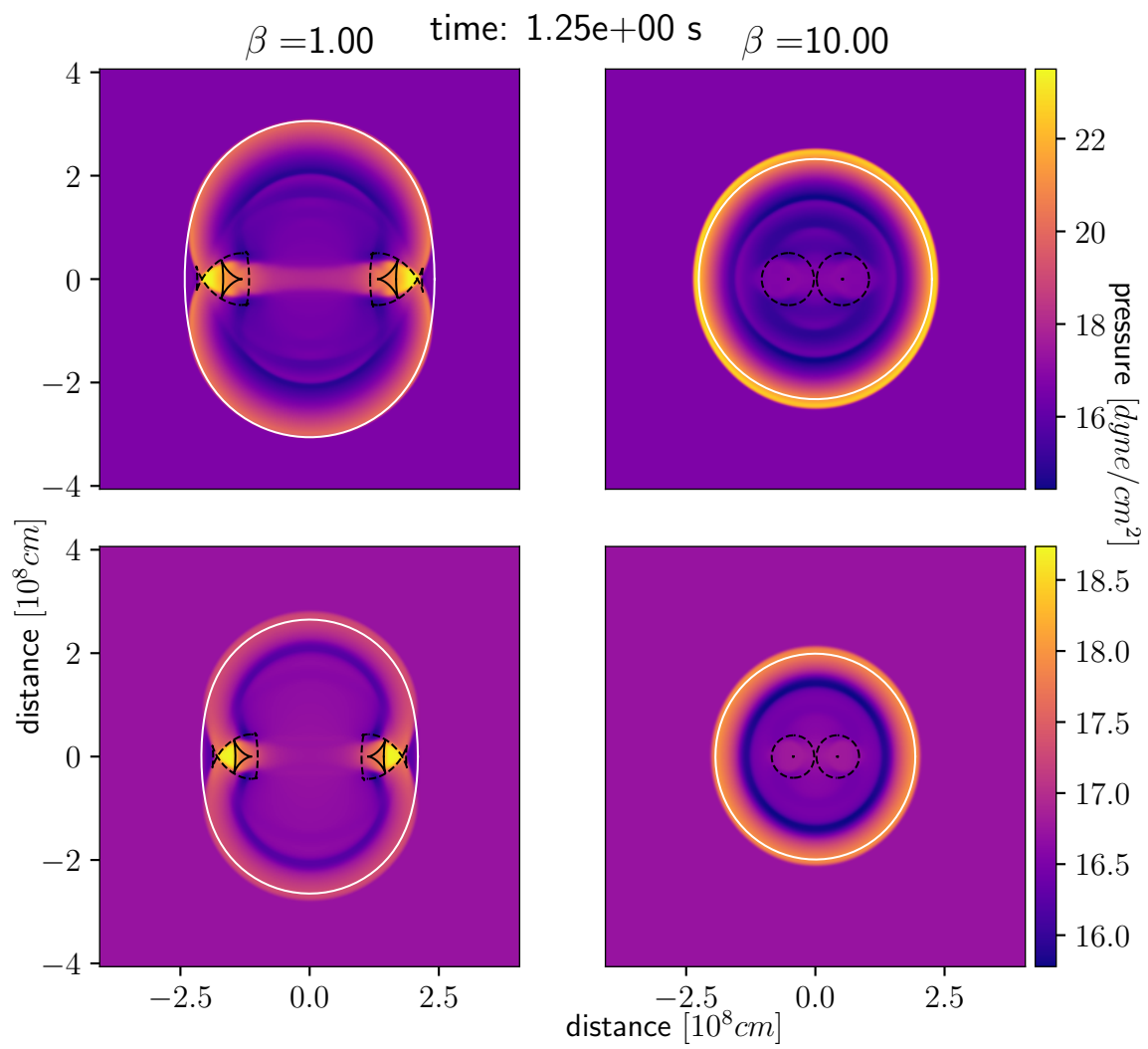


Figure 7: Plots of the pressure wave after 1.25 time units for different values of β . The white dotted line represents the theoretical position of the fast mode magneto-acoustic wave. The black solid lines are the parts of the group speed diagram corresponding to the slow-mode magnetoacoustic wave, and the black dotted lines are the initial condition boundary. This forms a boundary within which the slow mode wave propagates.

Figure 8: Same as fig. 7 but for different β values.

4 Cornal hole

In this section we study the interaction of a so called "coronal hole" with an MHD wave as introduced in the paper [coronal-hole] by A.N. Afanasyev and A. N. Zhukov. A coronal hole is a region in the coronal with much lower density and a lower temperature than the surrounding area. A the coronal hole was simulated in 2.5d, assuming that the variables do not depend on z but the z -components of vectors do not need to be zero. An ideal equation of state is assumed, this gives the following relation between density, temperature and pressure:

$$nk_B T = p \quad (38)$$

The total pressure p^T is given by [REF], from there the magnitude of the magnetic field is calculated as follows (expressions for code units):

$$B = \sqrt{2(p^T - p)} \quad (39)$$

The total pressure inside and outside the coronal hole is kept in equilibrium by changing the magnitude of the magnetic field accordingly.

The parameters for the coronal hole are the same as in [coronal-hole]. The physical size of the domain is a square with sidelength $2 \times 10^{11} \text{ cm}$, the grid used for the simulation has 1024 by 1024 gridpoints. As a model for the number density and temperature the following was used:

$$\begin{aligned} n(r) &= n_{out} - (n_{out} - n_{in}) \exp(-(r/d)^8) \\ T(r) &= T_{out} - (T_{out} - T_{in}) \exp(-(r/d)^8) \end{aligned} \quad (40)$$

r represents the distance from the center of the hole and d the characteristic size of the hole. The parameters n_{out}, n_{in}, T_{out} and T_{in} are respectively the plasma number density outside and inside the hole, the temperature outside and the temperature inside the hole. The magnetic field has zero x and y component and the z component is calculated according to eq. (39). The total pressure is calculated by fixing a value B_{out} for the magnitude of the magnetic field far away from the hole, and calculated using [ref]. As a counterpart to the coronal hole model a coronal plume model was considered as well, again based on [coronal-hole]. Here the density outside the plume is a lot lower than the density inside. The parameter values for both models can be found in fig. 8. In fig. 9 and fig. 10 the value of some impotant quantities at $t = 0$ are shown along a section through the center of the hole or plume respectively.

Parameter	Coronal hole	Coronal plume
n_{out}	$1.0 \times 10^9 \text{ cm}^{-3}$	$1.0 \times 10^8 \text{ cm}^{-3}$
n_{in}	$1.0 \times 10^8 \text{ cm}^{-3}$	$1.0 \times 10^9 \text{ cm}^{-3}$
T_{out}	$1.5 \times 10^6 \text{ K}$	$1.5 \times 10^6 \text{ K}$
T_{in}	$1.0 \times 10^6 \text{ K}$	$1.0 \times 10^6 \text{ K}$
d	$1.5 \times 10^{10} \text{ m}$	$1.0 \times 10^{10} \text{ m}$
B_{out}	4.0 G	3.0 G
v_m	50 km s ⁻¹	125 km s ⁻¹
s_1	20 s	60 s
s_2	16 s	50 s

Table 1: Parameter values taken from [coronal-hole]. The values used for the initial condition of the coronal hole and coronal plume models.

For the nonlinear wave driver the velocity along x was perturbed at the left boundaryi. To smoothly transition from 0 to a certain max velocity v_m , stay at this velocity for some time and smoothly go back to 0 a combination of two hyperbolic tangents is used in the following formula:

$$v_x(t) = v_m \tanh\left(\frac{t}{s_1}\right) - \frac{v_m}{2} \left(\tanh\left(\frac{t - T_0}{s_2}\right) + 1 \right) \quad (41)$$

The parameters s_1 and s_2 control the steepness of the transition from $v = 0$ to $v = v_m$. T_0 controls the time when the velocity drops back from v_m to 0, at $t = 0$ the velocity starts increasing immediately. This wave propagates with the speed of a fast magnetoacoustic wave transverse to the magnetic field (in the z -direction). From fig. 9 and fig. 10 it is clear that this speed is a lot higher in the case of the coronal plume than in the coronal hole model (about 2.5 times). To get a wave of the same physical width in both simulations, we use a shorter wave pulse in the coronal plume model with slightly steeper edges and higher maximum velocity. The parameters for the waves can also be found in fig. 8.

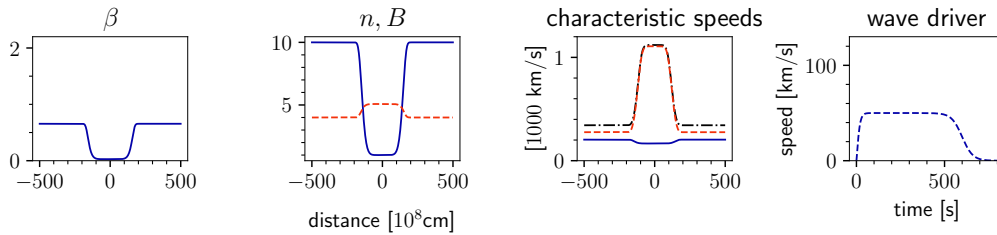


Figure 9: Sections of the initial condition for the *coronal hole* model. *First plot*: plasma beta as given by [REF], dimensionless quantity. *Second plot*: the full blue line is the plasma number density in 10^8 cm^{-3} . The red dashed line is the magnetic field in Gauss. *Third plot*: full line is the sound speed v_s , dashed red line the Alfvén speed v_a and the dash-dotted black line the fast magnetoacoustic speed v_+ . *Last plot*: speed profile of the wave driver used. Adapted from [coronal-hole]

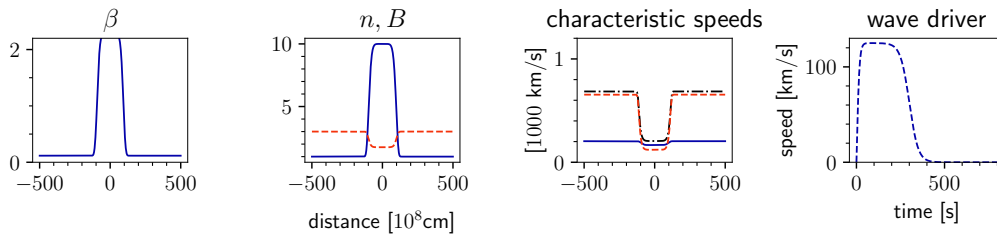


Figure 10: Same as fig. 9 but for the *coronal plume* model.

In fig. 11 a couple of density profiles of the simulation are plotted.

- coronal hole
 - discuss wave transmission through hole (fast) and form of transmission (initial shockfront, higher density, drops back down)
 - discuss shift in position
 - discuss rarefaction wave and diffracted waves
- coronal plume
 - reflected wave
 - transmitted wave (slower) and reflection inside plume + secondary transmitted waves
 - caustic focussing effects (high density \rightarrow energy \rightarrow observations?)
 - shift/deforming of structure
 - deformation of wave

General: add more background on how the simulations were done and how the data was condensed into plots. e.g. multiple attempts with different parameters, making animations to spot patterns and

general behaviour, rerunning with higher detail... (for example: more frames required to capture fast wave inside hole)

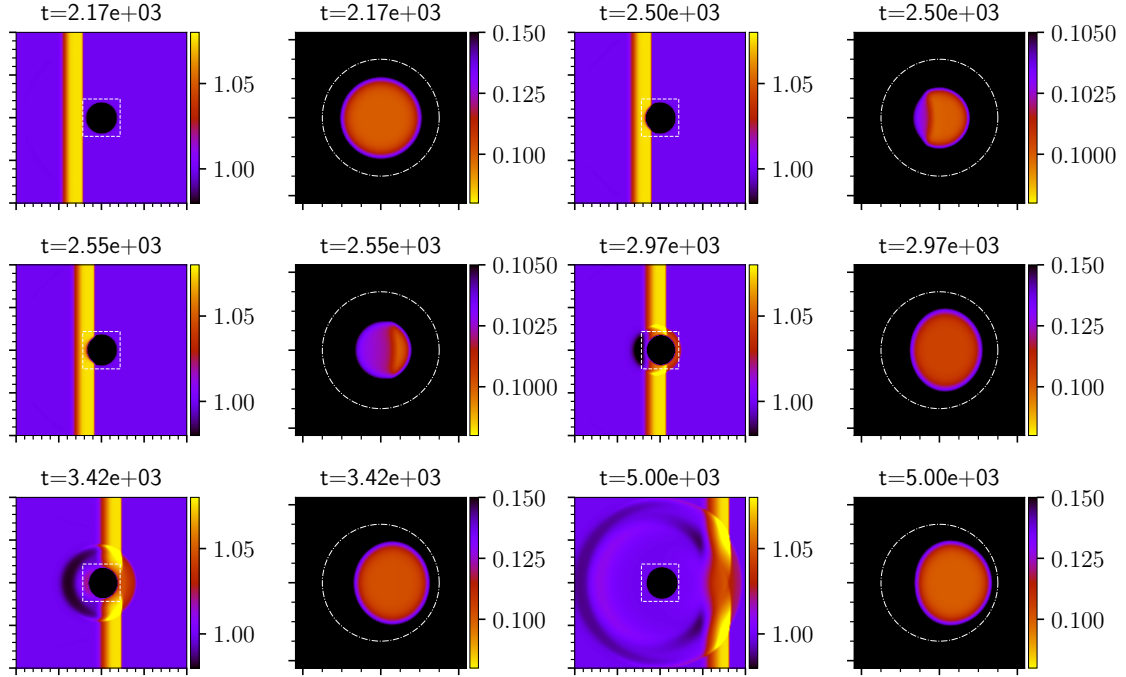


Figure 11: Plots of the density profile of the *coronal hole model* for different times. The plots in the first and third column cover the complete domain. The plots in the second and last column are zooms on the plume. The domain covered is the white box in the plots to the left. The density is measured in 10^9 cm^{-3} . The white circle has the characteristic width d as diameter. In the second and third pair of plots, the density range for the right plot is taken a lot more narrow to highlight the wave transmitted through the coronal hole.

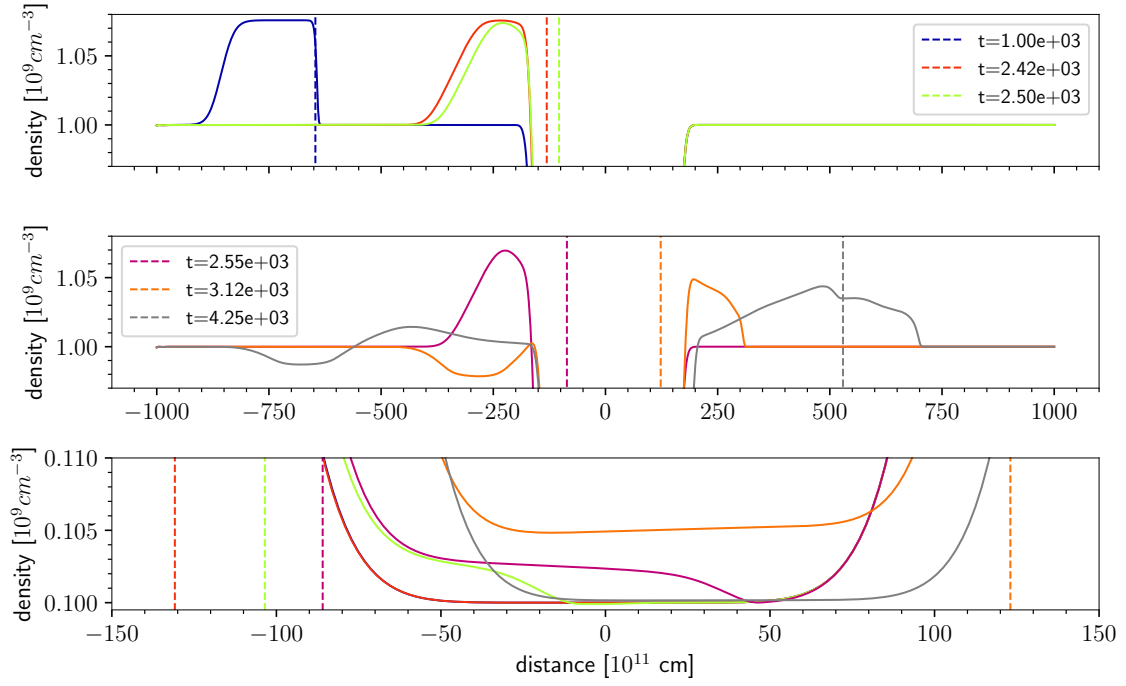


Figure 12: Density profiles along a cut, parallel to the direction of propagation of the wave, through the center of the *coronal hole* at different times. The vertical dashed lines show the position of the wavefront at the bottom edge of the simulation domain.

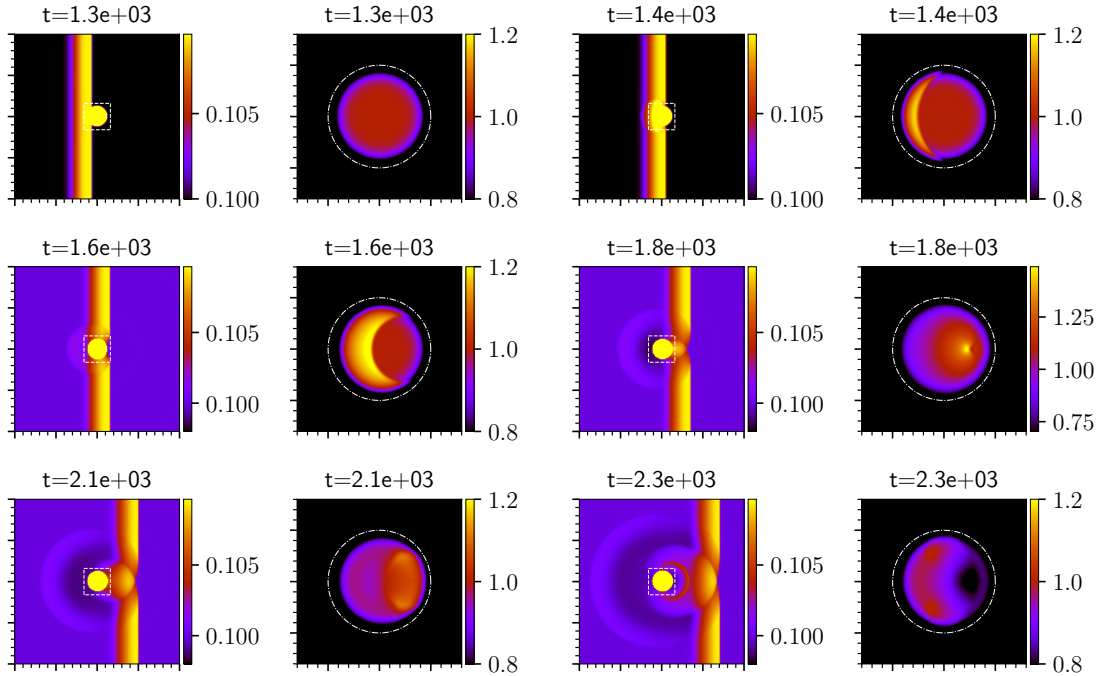


Figure 13: Plots of density profiles for the *coronal plume model*. Same conventions used as in fig. 11

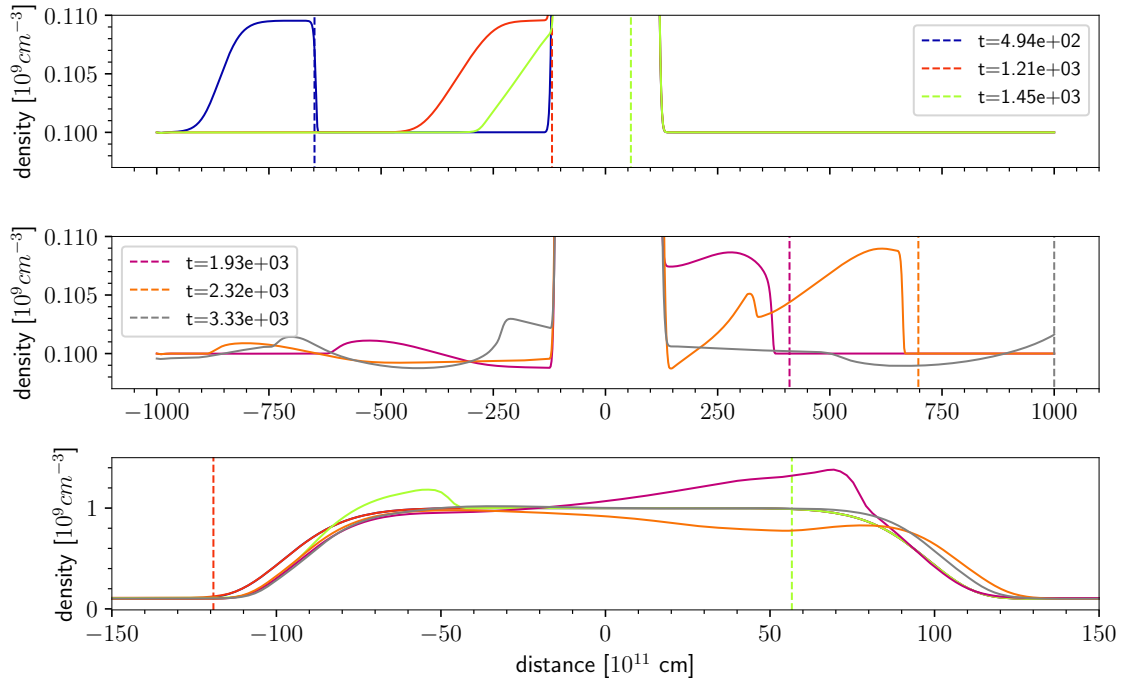


Figure 14: Density profiles along a cut through the center of the *coronal plume* at different times, along the direction of propagation of the waves. The vertical dashed lines show the position of the wave at the bottom edge of the simulation domain.

add discussion of simulation results: refraction effects

add short discussion of coronal plume